Power Congestion Management of a sub-Transmission Area Power Network using Partial Renewable Power Curtailment via MPC

Duc-Trung Hoang, Sorin Olaru, Alessio Iovine, Jean Maeght, Patrick Panciatici, Manuel Ruiz

Power Congestion Management of a sub-Transmission Area Power Network using Partial Renewable Power Curtailment via MPC

Duc-Trung Hoang[1], Sorin Olaru[1], Alessio Iovine[1], Jean Maeght[2], Patrick Panciatici[2] and Manuel Ruiz[2]

***Abstract*— Control systems dedicated to manage power transmission networks are facing design and deployment problems due to uncertainties and input time-delays, which may affect the overall system's performance and stability. To face situations due to the violations of the power lines thermal limits, the French Transmission System Operator (TSO) RTE aims to focus on splitting the entire system in sub-transmission areas (zones), and operate optimal management of battery devices and renewable production curtailments. The target of the present paper is to describe a time-delay model-based control approach for managing the electric power flow in sub-transmission zones dealing with model uncertainties while ensuring problem feasibility. Simulations on a case study of industrial interest validate the proposed method.**

***Index Terms*— Power transmission network, constrained model predictive control, partial power curtailment, energy storage, time-delay system.**

I. Introduction

Due to its competitive cost and positive environmental impact, the utilisation of renewable power is increasing worldwide. However, its introduction complicates power systems operation and management, and affects their stability, as small fluctuations in distributed generation may impact power systems' performance. In order to deal with the increasing difficulties related to power congestion on transmission lines, the French Transmission System Operator (TSO) RTE is focusing on innovative approaches to manage the transmission grid [1]. A main solution concerns the possibility to use storage devices and renewable power curtailments to manage sub-transmission areas (zones) via optimal control approaches.

To the purpose of considering a broader range of decisions with respect to the currently allowed ones, a time-delay model describing partial power curtailment possibilities is introduced in [2]. The considered model is based on Power Transfer Distribution Factor (PTDF) (see [3], [4]) and extends previous modeling that only allowed on/off decisions on power curtailment (see [5], [6]). In [7], preliminary results on the possibility to use model-based optimal control strategies to manage sub-transmission area congestion situations are carried out for a simplified model without delays. The present paper considers the modeling with time-delays, and provides a controllability analysis with respect to the saturation effects of the control inputs. Moreover, ad hoc strategies to ensure problem feasibility and to correctly prioritize the available control action are implemented. The target of the current work is the utilisation of real-time control strategy as Model Predictive Control (MPC) [8] to operate on the storage devices and partially curtail power from renewables, whenever the constraints on the operation of power lines are violated. The main challange comes from the uncertainties due to the availability of only local information and unknown variations of the power generators affects the decision making.

The contribution of the present paper concerns the use of MPC with respect to an extended state space that is obtained by modeling the time-delayed system as a linear not-delayed one, while facing the challenges of dealing with model partial controllability, uncertainties and feasibility issues in the real-time optimization. We consider previous results on MPC for time-delay systems as [9], [10], [11]. In [9], the utilisation of a receding horizon control strategy via MPC for time delay systems is shown to be possible in case of known delays by using a LMI approach. In [10], the authors described the possibility to handle MPC strategies for time-varying state-delay systems with uncertainty and constrained control input, while [11] analyses different use of the past information on the prediction-based feedback structure. The present work builds on these concepts and additionally employs a relaxations of constraints whenever the problem feasibility or the uncertainty impose it. Indeed, although MPC is a successful tool to manage the control of constrained systems while offering guaranteed constraint results, the structural lack of controllability for the system and the saturation of the control inputs could lead to constraints violation in several prediction steps. Consequently, the optimal control problem would become infeasible in closed-loop. To handle this problem, we soften the constraints by adding some slack variables [12], a technique which is suitable with respect to the thermal limit of the transmission lines of the Power Network.

The proposed control approach is validated trough simulations in a industrial case study that considers a sub-transmission area close to Dijon, France (see Figure 1). It is composed by six nodes with loads, generators and a battery. The simulation tool MATPOWER (see [13]) describing the

*This work was carried out within the CPS4EU project, which has received funding from the ECSEL Joint Undertaking (JU) under grant agreement No 826276. The JU receives support from the European Union's Horizon 2020 research and innovation programme and France, Spain, Hungary, Italy, Germany. The proposed results reflect only the authors' view. The JU is not responsible for any use that may be made of the information the present work contains.

[1] Laboratory of Signals and Systems (L2S), *CentraleSupélec, Paris-Saclay University*, Gif-sur-Yvette, France {trung.hoang-duc, sorin.olaru, alessio.iovine}@centralesupelec.fr

[2] French Transmission System Operator (TSO), *Réseau de Transport d'Électricité* (RTE), Paris, France {jean.maeght, patrick.panciatici, manuel.ruiz}@rte-france.com

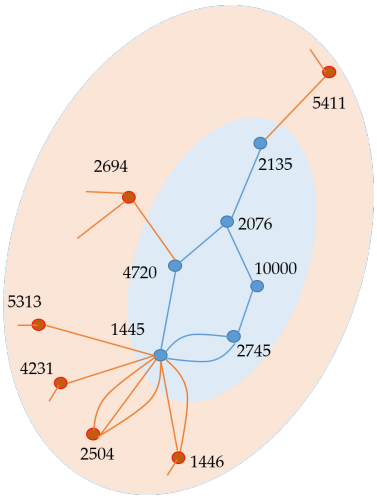

Fig. 1. The considered zone (blue nodes) and its connection to the entire power network (red nodes). The power flow interaction among the blue nodes and the red nodes is described as an uncontrolled generated/absorbed power and thus assimilated as disturbances in the decision making process.

full French transmission network (see [14]) is used to simulate the power transmission lines under various scenarios, using real data for renewable power generation. Target of the MPC tuning is to appropriately model and control the generated power on the nodes and their influence on the branches of the electrical transmission model.

The paper is organized as follows. Section II introduces the considered control-oriented modeling and Section III describes the MPC setting. Simulations validating the control approach are carried out in Section IV, while concluding remarks are outlined in Section V.

Notation:

- $\mathcal{Z}^N$ is the set of nodes in the considered zone; n^N is its cardinality. P_n^T is the power generated in the transmission network flowing from the external network to the node $n \in \mathcal{Z}^N$ of the zone of interest.
- $\mathcal{Z}^C \subset \mathcal{Z}^N$ is the set of nodes where the curtailment of the generated power is allowed; n^C is its cardinality. P_n^G is the generated power, while P_n^C is the curtailed one at node $n \in \mathcal{Z}^C$. P_n^A is the available renewable power that can be generated each sampling time.
- $\mathcal{Z}^B \subset \mathcal{Z}^N$ is the set of nodes with a battery; n^B is its cardinality. P_n^B is the power injected from the battery on node $n \in \mathcal{Z}^C$, while E_n^B describes the battery energy at the same node.
- $\mathcal{Z}^L \subset \{(i,j) \in \{1,...,n^N\} \times \{1,...,n^N\}\}$ is the set of power lines in the zone; n^L is its cardinality. F_{ij} represents the power flow on the line ij.

The operator $diag$ describes a diagonal matrix composed by the considered elements. The operator col produces a single column vector composed by the aggregation of other vectors. That is, given m vectors $s_i \in \mathbb{R}^n$, $i = 1, ..., m$, the resulting vector $s = col[s_i], i = 1, 2, \ldots, m$, will be:

$$s = col[s_i] = [\ s_1^T\ \ s_2^T\ \ ...\ \ s_m^T\ ]^T \in \mathbb{R}^{nm}. \tag{1}$$

II. Modeling

We consider a discrete-time linear system with delay describing the interaction within the transmission network based on PTDFs (see [2] for details on the modelling). The following working hypothesis are considered:

1) each generator produces the maximum available renewable power or the maximum allowed one;
2) only a higher level controller can decrease the power curtailment set-points. For this reason, the proposed controller deals only with curtailment increase;
3) the State of Charge (SOC) of the battery is updated each second by a SCADA system. Together with the considered high voltage, these short time intervals with respect to longer ones taken here into account for control purposes, both sampling and prediction horizon, allow to neglect losses due to the battery system (conversion, cooling and transformers). A different control level is supposed to manage the SOC with respect to longer time horizons [15];
4) the loads are constant.

The state variables of the energy transmission are: the power flows on the lines F_{ij}, the curtailed power P_n^C and the battery power output P_n^B, respectively, the battery energy E_n^B, and the generated power P_n^G. The control (delayed) inputs are the power variations ΔP_n^B and ΔP_n^C. The disturbance ΔP_n^T is unknown, as it represents the power variations on the nodes outside the operated zone. Finally, the power variation ΔP_n^G of the generated power P_n^G is a filtered disturbance acting on the system. It is known at instant k based on the state, control input and context information within the zone (available power). We suppose the available power P_n^A is communicated to the TSO at each sampling time, together with the power variation ΔP_n^A. Consequently, the value of ΔP_n^G is implicitly defined with respect to the communicated values of P_n^A, ΔP_n^A, and the stored value of P_n^G with respect to P_n^C.

The dynamical model is:

$$\begin{cases} F_{ij}(k+1) = & F_{ij}(k) + \sum_{n\in\mathcal{Z}^B} b_{ij}^n \Delta P_n^B(k-d) \\ & + \sum_{n\in\mathcal{Z}^C} b_{ij}^n \left[\Delta P_n^G(k) - \Delta P_n^C(k-\tau)\right] \\ & + \sum_{n\in\mathcal{Z}^N} b_{ij}^n \Delta P_n^T(k),\ \forall\ (ij) \in \mathcal{Z}^L \\ P_n^C(k+1) = & P_n^C(k) + \Delta P_n^C(k-\tau),\ \forall\ n \in \mathcal{Z}^C \\ P_n^B(k+1) = & P_n^B(k) + \Delta P_n^B(k-d),\ \forall\ n \in \mathcal{Z}^B \\ E_n^B(k+1) = & E_n^B(k) - Tc_n^B[P_n^B(k) + \Delta P_n^B(k-d)], \\ & \forall\ n \in \mathcal{Z}^B \\ P_n^G(k+1) = & P_n^G(k) + \Delta P_n^G(k) - \Delta P_n^C(k-\tau), \\ & \forall\ n \in \mathcal{Z}^C \end{cases} \tag{2}$$

where b_{ij}^n are constant parameters given by PTDF computation, and c_n^B are constant power reduction factor for the batteries, and $d \geq 1$ and $\tau \geq 1$ are operational time delays due to the delayed control actions on battery power output and power curtailment for the generators, respectively. We consider the batteries to act faster with respect to the

possibility to curtail renewable power, and consequently $\tau \geq d$.

In particular, the term $\Delta P_n^G(k)$, is defined as

$$\Delta P_n^G(k) = \min\left(f_n^G(k), g_n^G(k)\right), \tag{3}$$

with

$$f_n^G(k) = P_n^A(k) + \Delta P_n^A(k) - P_n^G(k) + \Delta \hat{P}_n^C(k-\tau), \tag{4}$$

$$g_n^G(k) = \overline{P}_n^G - P_n^C(k) - P_n^G(k). \tag{5}$$

where $\overline{P}_n^G > 0$ is the maximum installed capacity of the power that can be generated by the n renewable power plant, with $n \in \mathcal{Z}^C$, and the value of $\Delta \hat{P}_n^C(k)$ is defined in the following. According to this, the proposed modeling allows for the possibility to pre-compute the term $\Delta P_n^G(k)$, based on values of $P_n^A(k)$, $P_n^G(k)$, $P_n^C(k)$, $\Delta P_n^A(k)$ and $\Delta P_n^C(k)$, while maintaining the system linear via the offline computation of the $\min(.)$ and consequently reducing the computational effort of dedicated model-based predictive control laws. The main drawback is related to the term $\Delta \hat{P}_n^C(k)$. Whenever this is an independent variable at the pre-computation time of sampling instant k, i.e. whenever $\Delta \hat{P}_n^C(k) = \Delta P_n^C(k)$, then model (2) is implicitly nonlinear.

To avoid this implicit dependence in (2), we target to purposely consider a predicted value in (4), e.g. $\Delta \hat{P}_n^C(k-\tau) = 0$, and dissociate it from the actual selection of $\Delta P_n^C(k-\tau)$, which is the control input to be fixed at time $k-\tau$. The linearity of the prediction model is preserved and its evolution can be corrected once $\Delta P_n^C(k-\tau)$ is chosen. This mechanism implies a model mismatch in between the prediction and the correction phase, whenever $\Delta P_n^C(k-\tau) \neq \Delta \hat{P}_n^C(k-\tau)$. However, since the goal is to minimise the power curtailment, by selecting $\Delta \hat{P}_n^C(k-\tau) = 0$ we reduce the impact of the model mismatch.

To describe the model in a compact form, we define:

$$F = col[F_{ij}],\ \forall\ (i,j) \in \mathcal{Z}^L; \tag{6a}$$

$$P^C = col[P_n^C],\ \Delta P^C = col[\Delta P_n^C],\ \forall\ n \in \mathcal{Z}^C; \tag{6b}$$

$$P^B = col[P_n^B],\ \forall\ n \in \mathcal{Z}^B; \tag{6c}$$

$$E^B = col[E_n^B],\ \Delta P^B = col[\Delta P_n^B],\ \forall\ n \in \mathcal{Z}^B; \tag{6d}$$

$$\Delta P^T = col[\Delta P_n^T],\ \forall\ n \in \mathcal{Z}^N; \tag{6e}$$

$$P^G = col[P_n^G],\ \Delta P^G = col[\overline{P}_n^G],\ \forall\ n \in \mathcal{Z}^C \tag{6f}$$

According to (6a)-(6f), the resulting linear system is described as

$$\begin{aligned} x(k+1) =& Ax(k) + B_C u_C(k-\tau) + B_B u_B(k-d) \\ &+ D_w w(k) + D_\zeta \zeta(k) \end{aligned} \tag{7}$$

where

$$x(k) = [F(k)\ \ P^C(k)\ \ P^B(k)\ \ E^B(k)\ P^G(k)]^T, \tag{8}$$

$$u_C(k) = \Delta P^C(k),\quad u_B(k) = \Delta P^B(k), \tag{9}$$

$$w(k) = \Delta P^G(k),\quad \zeta(k) = \Delta P^T(k), \tag{10}$$

$$A = \begin{pmatrix} \mathbb{1}_{\mathbf{nL}\times\mathbf{nL}} & \mathbb{0}_{\mathbf{nL}\times\mathbf{nC}} & \mathbb{0}_{\mathbf{nL}\times\mathbf{nB}} & \mathbb{0}_{\mathbf{nL}\times\mathbf{nB}} & \mathbb{0}_{\mathbf{nL}\times\mathbf{nC}} \\ \mathbb{0}_{\mathbf{nC}\times\mathbf{nL}} & \mathbb{1}_{\mathbf{nC}\times\mathbf{nC}} & \mathbb{0}_{\mathbf{nC}\times\mathbf{nB}} & \mathbb{0}_{\mathbf{nC}\times\mathbf{nB}} & \mathbb{0}_{\mathbf{nC}\times\mathbf{nC}} \\ \mathbb{0}_{\mathbf{nB}\times\mathbf{nL}} & \mathbb{0}_{\mathbf{nB}\times\mathbf{nC}} & \mathbb{1}_{\mathbf{nB}\times\mathbf{nB}} & \mathbb{0}_{\mathbf{nB}\times\mathbf{nB}} & \mathbb{0}_{\mathbf{nB}\times\mathbf{nC}} \\ \mathbb{0}_{\mathbf{nB}\times\mathbf{nL}} & \mathbb{0}_{\mathbf{nB}\times\mathbf{nC}} & -A_b & \mathbb{1}_{\mathbf{nB}\times\mathbf{nB}} & \mathbb{0}_{\mathbf{nB}\times\mathbf{nC}} \\ \mathbb{0}_{\mathbf{nC}\times\mathbf{nL}} & \mathbb{0}_{\mathbf{nC}\times\mathbf{nC}} & \mathbb{0}_{\mathbf{nC}\times\mathbf{nB}} & \mathbb{0}_{\mathbf{nC}\times\mathbf{nB}} & \mathbb{1}_{\mathbf{nC}\times\mathbf{nC}} \end{pmatrix}, \tag{11}$$

$$B_C = \begin{pmatrix} -M_c \\ \mathbb{1}_{\mathbf{nC}\times\mathbf{nC}} \\ \mathbb{0}_{\mathbf{nB}\times\mathbf{nC}} \\ \mathbb{0}_{\mathbf{nB}\times\mathbf{nC}} \\ -\mathbb{1}_{\mathbf{nC}\times\mathbf{nC}} \end{pmatrix},\quad B_B = \begin{pmatrix} M_b \\ \mathbb{0}_{\mathbf{nC}\times\mathbf{nB}} \\ \mathbb{1}_{\mathbf{nB}\times\mathbf{nB}} \\ -A_b \\ \mathbb{0}_{\mathbf{nC}\times\mathbf{nB}} \end{pmatrix}, \tag{12}$$

$$D_w = \begin{pmatrix} M_c & \mathbb{0}_{\mathbf{nC}\times\mathbf{nC}} & \mathbb{0}_{\mathbf{nB}\times\mathbf{nC}} & \mathbb{0}_{\mathbf{nB}\times\mathbf{nC}} & \mathbb{1}_{\mathbf{nC}\times\mathbf{nC}} \end{pmatrix}^T, \tag{13}$$

$$D_\zeta = \begin{pmatrix} M_t & \mathbb{0}_{\mathbf{nC}\times\mathbf{nN}} & \mathbb{0}_{\mathbf{nB}\times\mathbf{nN}} & \mathbb{0}_{\mathbf{nB}\times\mathbf{nN}} & \mathbb{0}_{\mathbf{nC}\times\mathbf{nN}} \end{pmatrix}^T, \tag{14}$$

with $A_b = diag[Tc_n^B],\ \forall\ n \in \mathcal{Z}^B$, and M_c, M_b and M_t that are composed by the elements b_{ij}^n of the PTDF matrix described in (2). The k^{th} line in these matrices corresponds to the PTDF of the k^{th} line of F_{ij} at nodes where generation can be curtailed, at nodes where a battery is installed or at nodes where the injections may vary, respectively.

We remark that reactive voltage aspects are not considered in this work. This modeling is adapted to identify in real-time the need for acting on curtailment or storage charge/discharge. Alternate Current (AC) feasibility is a consequence of online updates of $cos(\phi)$ from active power and current real-time measurements, where $cos(\phi)$ is the usual power/current ratio at each bus.

A. Controllability and structural analysis

Using the controllability tests for the state-space dynamics (7), the direct conclusion is that pairs (A, B_C) and (A, B_B) are not fully controllable. This first conclusion does not bring important information as long as parts of the state vector are affected in a similar manner (linear dependency) by the control signals as for example the curtailed power. A more insightful information comes from the analysis of the dynamics of the flow components in (6a) which are subject to constraints on their evolution. It becomes apparent that full controllability is not granted for these components of the state dynamics which are disconnected from the other states. The flow dynamics can be thus considered to be underactuated in the sense that not all the configurations of flows can be reached from an arbitrary initial state.

Few remarks can be made:

i The sub-matrix corresponding to the flow evolution being the identity, the flow evaluations can be analysed in terms of the controllable subspace which is span by the columns of the matrices B_C and B_B. In particular, in case of co-location of the batteries with a subset of the production sites, the controllability index is the rank of B_C. When the battery is collocated with the production site (a node of the network), the columns of B_B are representing a subset of the columns of B_C. However, the batteries are associated with indefinite sign control signals while the curtailment is restricted to positive control signals.

ii The saturation of the battery capacity will impact the flow dynamics. In the case of saturation of one of the batteries, the respective column of the B_B matrix becomes zero, thus impacting the controllability of the flow dynamics.

iii The dimension of the controllable subspace is strictly smaller than the dimension of the flows subspace in the state space. The argument for this last property is related to the fact that structurally, the number of columns in the B_C is related to the number of nodes in the transmission graph while the dimension of the flow (state) vector is related to the number of arches. The later one being strictly greater than the first one, the fully controllability cannot be achieved (due to the property i. above).

iv The curtailment signal is monotonically increasing. This constraint can be further analyzed by means of the signs of the PTDF coefficients. E.g. if one of the branches has all associated coefficients positive (negative), then the curtailment impact is unilateral on the flow of the branch.

v The lack of complete controllability is not compromising the constraint admissibility of the flow dynamics under the assumptions that its initialization is done within the controllable subspace.

B. Extended state

In order to deal with the known actuator delays $\tau \geq 1$ and $d \geq 1$, we define an extended state $\tilde{x}$ as

$$\tilde{x}(k) = [x(k)\, u_C(k-\tau)\, ...\, u_C(k-1)\, u_B(k-d)\, ...\, u_B(k-1)]^T. \tag{15}$$

The resulting dynamical system is as follows:

$$\begin{aligned}\tilde{x}(k+1) &= \tilde{A}\tilde{x}(k) + \\ &+ \underbrace{\begin{bmatrix} \tilde{B}_C\ \tilde{B}_B \end{bmatrix}}_{\tilde{B}} \underbrace{\begin{bmatrix} u_C(k) \\ u_B(k) \end{bmatrix}}_{u(k)} + \underbrace{\begin{bmatrix} \tilde{D}_w\ \tilde{D}_\zeta \end{bmatrix}}_{\tilde{D}} \underbrace{\begin{bmatrix} w(k) \\ \zeta(k) \end{bmatrix}}_{\eta(k)}\end{aligned} \tag{16}$$

where, for the particular case $d = 1$ and $\tau > 1$, the matrices are

$$\underbrace{\begin{pmatrix} A & B_C & \mathbb{0} & \dots & \mathbb{0} & B_B & \mathbb{0} \\ \mathbb{0} & \mathbb{0} & \mathbb{1} & \mathbb{0} & \mathbb{0} & \mathbb{0} & \mathbb{0} \\ \vdots & \mathbb{0} & \mathbb{0} & \ddots & \mathbb{0} & \vdots & \vdots \\ \mathbb{0} & \mathbb{0} & \dots & \mathbb{0} & \mathbb{1} & \mathbb{0} & \mathbb{0} \\ \mathbb{0} & \mathbb{0} & \mathbb{0} & \mathbb{0} & \mathbb{0} & \mathbb{0} & \mathbb{0} \\ \mathbb{0} & \mathbb{0} & \mathbb{0} & \mathbb{0} & \mathbb{0} & \mathbb{0} & \mathbb{1} \\ \mathbb{0} & \mathbb{0} & \mathbb{0} & \mathbb{0} & \mathbb{0} & \mathbb{0} & \mathbb{0} \end{pmatrix}}_{\tilde{A}}; \underbrace{\begin{pmatrix} \mathbb{0} \\ \mathbb{0} \\ \vdots \\ \mathbb{0} \\ \mathbb{1} \\ \mathbb{0} \\ \mathbb{0} \end{pmatrix}}_{\tilde{B}_C}; \underbrace{\begin{pmatrix} \mathbb{0} \\ \mathbb{0} \\ \vdots \\ \mathbb{0} \\ \mathbb{0} \\ \mathbb{0} \\ \mathbb{1} \end{pmatrix}}_{\tilde{B}_B}; \tag{17}$$

$$\tilde{D}_w = \begin{pmatrix} D_w & \mathbb{0} & \dots & \mathbb{0} & \mathbb{0} & \mathbb{0} & \mathbb{0} \end{pmatrix}^T; \tag{18}$$

$$\tilde{D}_\zeta = \begin{pmatrix} D_\zeta & \mathbb{0} & \dots & \mathbb{0} & \mathbb{0} & \mathbb{0} & \mathbb{0} \end{pmatrix}^T. \tag{19}$$

The matrices $\mathbb{1}$ and $\mathbb{0}$ have appropriate dimensions with respect to the state $\tilde{x}$ size, and to the delays τ and d. The proposed not-delayed system in (16) is equivalent to the delayed one in (7).

III. Control via MPC

Target of this Section is to describe how we apply MPC to the dynamical model in (16) by leveraging the available degrees of freedom given by the possibilities to act on the storage power outputs $u_B(k)$ and on the power curtailment $u_C(k)$. The real-time decisions on the curtailment and battery storage are to be selected within the feasible domain (imposed by the physical constraints on the power flow), and according to the uncertanties due to renewable power production and model mismatch. We remark that the considered prediction horizon is higher than the maximum delay τ.

A. Feedback control strategy description

In order to monitor the uncertainties, we list the available information at each time k:

- the power flows on the lines $F_{ij}(k)$ between the nodes of the considered zone can be measured or estimated;
- the information on power curtailment $P_n^C(k)$ is known, since it is based on the past congestion management decisions and the maximal productions;
- the information on battery power output $P_n^B(k)$ is considered deterministic, as it is operated based on the battery storage control signals, and can be matched with the effective measurements on the battery power output;
- the battery energy $E_n^B(k)$ can be directly computed with respect to the battery power output;
- the generated/consumed power in each of the nodes is the sensitive quantity in terms of information handling. As discussed in the previous section, it builds on power available (measured in the past but not available at time instant k), the maximal power on the nodes and decisions on power curtailment (affected by operational delays).

In order to have a clear picture of the relationship between the available information, the uncertainty and the decision making, let us introduce more details on the propagation of the uncertainties along the predictions. At each sampling time k, the uncertainties relies on the evolution of the generated power P_n^G for each node, and are described by:

$$\Delta P_n^G(k) = \Delta P_n^G(\Delta P_n^A(k), \Delta P_n^C(k-\tau)).$$

Clearly, the decision on the power curtailment is subject to uncertainty as long as one cannot exploit the aposteriori information. Thus $\Delta P_n^G(k)$ is unknown in:

$$\Delta P_n^C(k-\tau) = \Delta P_n^C(\Delta P_n^G(k)).$$

In these conditions one needs to rely on the predictions

$$\Delta P_n^C(k-\tau) = \Delta P_n^C(\Delta \hat{P}_n^G(k))$$

which can be further developed as

$$\Delta P_n^C(k-\tau) = \Delta P_n^C(\Delta \hat{P}_n^A(k), \Delta \hat{P}_n^C(k-\tau)).$$

When $\Delta P_n^A(k)$ is not available, the related uncertainty can be managed by extrapolations (for example, with alternatives for the estimation as $\Delta \hat{P}_n^A(k) = \Delta P_n^A(k-1)$ or $\Delta \hat{P}_n^A(k) =$

0). With respect to $\Delta\hat{P}_n^C(k)$, its impact can be handled based on a prediction-correction mechanism. In case of uncertainty at time instant k, its impact will be reiterated along the predictions as long as the same ingredients will have to be manipulated without prior information on ΔP_n^A and $\Delta\hat{P}_n^C$. Despite the jeopardizing effect of the uncertainty on the prediction, it has to be noticed that the control lever offered by the power curtailment is able to mitigate the uncertainty impact if the physical constraints are under threat, as long as there always exists a curtailment able to retrieve a level of power generation satisfying the constraints.

B. Mathematical formulation

Let us define the constant upper and lower bounds of each variable by the following notation: $L_{ij} > 0$, $\overline{P}_n^G > 0$, $\overline{P}_n^B > 0$, $\underline{P}_n^B < 0$, $\overline{E}_n^B > 0$, $\underline{E}_n^B > 0$. Then,

$$\overline{L} = col[L_{ij}], \forall\ (i,j) \in \mathcal{Z}^L; \tag{20a}$$

$$\underline{P}^B = col[\underline{P}_n^B],\ \overline{P}^B = col[\overline{P}_n^B],\ \forall\ n \in \mathcal{Z}^B; \tag{20b}$$

$$\underline{E}^B = col[\underline{E}_n^B],\ \overline{E}^B = col[\overline{E}_n^B],\ \forall\ n \in \mathcal{Z}^B; \tag{20c}$$

$$\overline{P}^G = col[\overline{P}_n^G],\ \forall\ n \in \mathcal{Z}^C. \tag{20d}$$

By assuming that the disturbances are bounded, the constraints would be:

$$-\overline{L} \leq F(k) \leq \overline{L},\quad \mathbb{0}_{\mathbf{n^C}\times\mathbf{1}} \leq P^C(k) \leq \overline{P}^G, \tag{21a}$$

$$\underline{P}^B \leq P^B(k) \leq \overline{P}^B,\quad \underline{E}^B \leq E^B(k) \leq \overline{E}^B, \tag{21b}$$

$$\mathbb{0}_{\mathbf{n^C}\times\mathbf{1}} \leq P^G(k) \leq \overline{P}^G,\quad \mathbb{0}_{\mathbf{n^C}\times\mathbf{1}} \leq \Delta P^C(k) \leq \overline{P}^G, \tag{21c}$$

$$\underline{P}^B - \overline{P}^B \leq \Delta P^B(k) \leq \overline{P}^B - \underline{P}^B, \tag{21d}$$

for all k. Let N be the prediction horizon, $d < \tau < N$. To ensure problem feasibility, we aim to relax the constraints related to the flow on the power lines for $F(k+i)$ when $i \in [0, \tau-1]$. According to the lack of degrees of freedom for controlling the system, we impose that $F(k+i)$ has no constraints for $i \in [0, d-1]$, and consider soft constraints for $i \in [d, \tau-1]$. Then, we introduce the softening slack variables $\varepsilon = col[\varepsilon_{ij}], \forall\ (i,j) \in \mathcal{Z}^L$, such that the flow on the branches may overtake some margins during the predictions:

$$-\overline{L}-\varepsilon(k+i) \leq F(k+i) \leq \overline{L}+\varepsilon(k+i),\ \ i \in [d, \tau-1]. \tag{22}$$

Finally, we consider the control inputs to be bounded:

$$\mathbb{0}_{\mathbf{n^C}\times\mathbf{1}} \leq u_C(k+i) \leq \overline{P}^G,\quad i \in [0, N-1]; \tag{23a}$$

$$\underline{P}^B - \overline{P}^B \leq u_B(k+i) \leq \overline{P}^B - \underline{P}^B,\quad i \in [0, N-1]. \tag{23b}$$

In order to consider the extended state, condition (23) is imposed also for the delayed control inputs, i.e.

$$\underbrace{\begin{pmatrix} \mathbb{0}_{\mathbf{n^C}\times\mathbf{1}} \\ \vdots \\ \mathbb{0}_{\mathbf{n^C}\times\mathbf{1}} \\ \underline{P}^B - \overline{P}^B \\ \vdots \\ \underline{P}^B - \overline{P}^B \end{pmatrix}}_{u_{\min}} \leq \begin{pmatrix} u_C(k-\tau) \\ \vdots \\ u_C(k-1) \\ u_B(k-d) \\ \vdots \\ u_B(k-1) \end{pmatrix} \leq \underbrace{\begin{pmatrix} \overline{P}^G \\ \vdots \\ \overline{P}^G \\ \overline{P}^B - \underline{P}^B \\ \vdots \\ \overline{P}^B - \underline{P}^B \end{pmatrix}}_{u_{\max}}. \tag{24}$$

To summarise, the constraints for the state $\tilde{x}$ in (15) are

$$\tilde{x}_{\min}(k+i) \leq \tilde{x}(k+i) \leq \tilde{x}_{\max}(k+i) \quad \forall\ i \in [0, N], \tag{25}$$

where the following three cases are considered, with respect to the i^{th} prediction step:

$*$) if $0 \leq i < d$:

$$\tilde{x}_{\min}(k+i) = [-\infty_{\mathbf{n^N}\times\mathbf{1}}\ \mathbb{0}_{\mathbf{n^C}\times\mathbf{1}}\ \underline{P}^B\ \underline{E}^B\ \mathbb{0}_{\mathbf{n^C}\times\mathbf{1}}\ u_{\min}^T]^T \tag{26a}$$

$$\tilde{x}_{\max}(k+i) = [\infty_{\mathbf{n^N}\times\mathbf{1}}\ \overline{P}^G\ \overline{P}^B\ \overline{E}^B\ \overline{P}^G\ u_{\max}^T]^T \tag{26b}$$

$*$) if $d \leq i < \tau$:

$$\tilde{x}_{\min}(k+i) = [-\overline{L} - \varepsilon(k+i)\ \mathbb{0}_{\mathbf{n^C}\times\mathbf{1}}\ \underline{P}^B\ \underline{E}^B\ \mathbb{0}_{\mathbf{n^C}\times\mathbf{1}}\ u_{\min}^T]^T \tag{27a}$$

$$\tilde{x}_{\max}(k+i) = [\overline{L} + \varepsilon(k+i)\ \overline{P}^G\ \overline{P}^B\ \overline{E}^B\ \overline{P}^G\ u_{\max}^T]^T \tag{27b}$$

$*$) if $\tau \leq i \leq N$:

$$\tilde{x}_{\min}(k+i) = [-\overline{L}\ \mathbb{0}_{\mathbf{n^C}\times\mathbf{1}}\ \underline{P}^B\ \underline{E}^B\ \mathbb{0}_{\mathbf{n^C}\times\mathbf{1}}\ u_{\min}^T]^T \tag{28a}$$

$$\tilde{x}_{\max}(k+i) = [\overline{L}\ \overline{P}^G\ \overline{P}^B\ \overline{E}^B\ \overline{P}^G\ u_{\max}^T]^T. \tag{28b}$$

A quadratic cost function is chosen to select a unique solution within the feasible domain by utilisation of soft constraints. It considers:

- set-point tracking; seldom used with lowest weighting to maintain the battery storage in the neighborhood of a *safety* pre-defined level.
- penalty on the control action related to the power curtailment by increasing weights.
- penalty on the control action related to the battery storage, to be weighted less than the ones on the power curtailment.
- introduction of softening constraints and extra cost for specific prediction step.

We consider weight functions $\lambda(i)$ and $\theta(i)$, where $\lambda(i)$ decreases with respect to time, whereas $\theta(i)$ increases according to i. To correctly model the choice to act on the battery first, we consider $\lambda(i) > \theta(i)$, $\forall\ i$. The function $\lambda(i)$ models the target to curtail at the really last needed sampling time. On the contrary, $\theta(i)$ describes the willingness to have a fast control action on the battery. A constant large enough parameter α is considered to avoid that the softening constraints may affect the optimization processing as well.

The cost function that considers the two actuator delays is

$$J(k) = J_1(k) + J_2(k) + J_3(k) \tag{29}$$

where

$$J_1(k) = \sum_{i=1}^{d-1} ||\tilde{x}(k+i) - \tilde{x}_r||^2_{\tilde{Q}} + \sum_{i=0}^{d-1} \lambda(i)||u_C(k+i)||^2_{R_C} + \sum_{i=0}^{d-1} \theta(i)||u_B(k+i)||^2_{R_B} \tag{30}$$

$$J_2(k) = \sum_{i=d}^{\tau-1} ||\tilde{x}(k+i) - \tilde{x}_r||^2_{\tilde{Q}} + \sum_{i=d}^{\tau-1} \lambda(i)||u_C(k+i)||^2_{R_C} + \sum_{i=d}^{\tau-1} \theta(i)||u_B(k+i)||^2_{R_B} + \sum_{i=d}^{\tau-1} \alpha||\varepsilon(k+i)||^2 \tag{31}$$

$$J_3(k) = \sum_{i=\tau}^{N} ||\tilde{x}(k+i) - \tilde{x}_r||^2_{\tilde{Q}} + \sum_{i=\tau}^{N-1} \lambda(i)||u_C(k+i)||^2_{R_C} + \sum_{i=\tau}^{N-1} \theta(i)||u_B(k+i)||^2_{R_B} \tag{32}$$

where $\tilde{Q}$, R_C, and R_B are semidefinite positive matrices with respect to the sizes $\tilde{x}, u_C$, and u_B, respectively, and $\tilde{x}_r$ is a reference vector for the state, mainly describing the reference power output and energy level of the battery..

Based on the cost function and on the physical constraints, the receding-horizon optimization problem is defined as:

$$\mathcal{O} = \arg \min_{u_C(k),u_B(k),\ldots,u_C(k+N-1),u_B(k+N-1)} J(k) \ in \ (29)$$
$$s.t. \ (16), (25) \ for \ k, \ldots k+N. \tag{33}$$

Along the prediction horizon, the value of $\Delta P_n^G(k)$ is computed with respect to the value of $\Delta P_n^A(k)$.

IV. Simulations

In this section, simulations are carried out for a specific case study of industrial interest. The considered zone has six nodes, seven branches, four generators among nodes, and one battery i.e: $n^L = 7$, $n^C = 4$ and $n^B = 1$. The power flow on each branch has limited minimum and maximum values as -45MW and 45MW, respectively, where the negative values describes the opposite direction of the power flow. The considered four power generators have minimum power equal to 0 MW and maximum installed power capacity of 78 MW, 66 MW, 54 MW, and 10 MW, respectively. Figure 2 depicts the evolution of the available power P^A over the considered simulation time; real data are used to take into account realistic wind power plants. The battery power output ranges from -10W to 10 MW. We consider the battery power output not to impact on the stored energy. The delay values for battery and curtailment actuators are $d = 1$ and $\tau = 7$, respectively, while the prediction horizon is $N = 10$. Simulation time is 600 s. The considered sampling time is 5 s. The control algorithms are implemented in MATLAB and YALMIP [16], while the used solver is GUROBI [17].

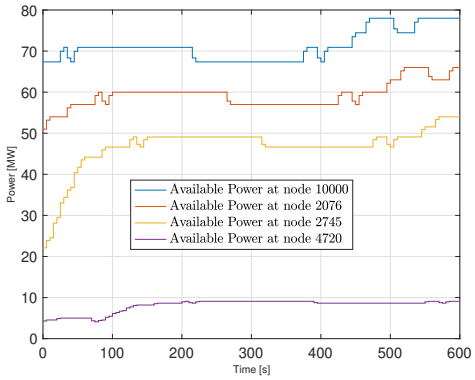

Fig. 2. The available powers for the four generators.

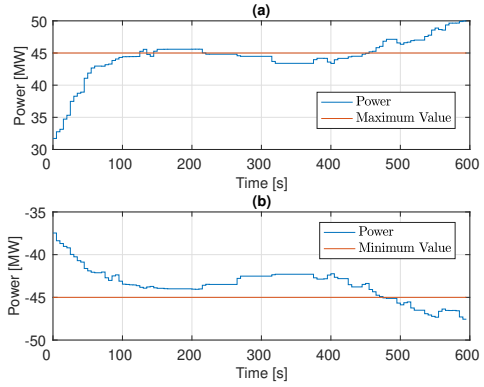

Fig. 3. The power flow on the branches in the open-loop simulation. (a): between buses 2745 and 1445. (b): between buses 2135 and 2076.

To emulate a real power transmission network, the function *runpf* of MATPOWER is used to simulate the AC power flow on the whole transmission network of the French electricity grid, that includes around 6000 buses [2], [14]. We remark that *runpf* will generate a succession of steady states; however, for the considered application it is possible to compare them to a time domain simulation. Figure 3 shows the power flow on two branches of the case of interest in case of open loop simulations, when no feedback correction mechanism is implemented via storage device utilisation or power curtailment. As clearly depicted, the power flow on the branch between buses 2745 and 1445, and on the branch between buses 2135 and 2076, violates the desired constraints. In the following of the section, we describe the closed loop simulation case with utilisation of the aforementioned controller.

We consider $\Delta P_n^G(k)$ to be constant over the prediction's interval from step $\tau+1$ to step N in MPC. On the contrary, to better analyse the effect of the mismatch of the real value of $\Delta P_n^G(k)$, we suppose the value of $\Delta P_n^A(k)$ is constant along the prediction horizon for a worst case scenario.

Since the only components of the state we want to consider for the optimisation are the ones related to the power curtailment and the battery power output, the matrix $\tilde{Q}$ is a diagonal one, and the elements corresponding to the variables

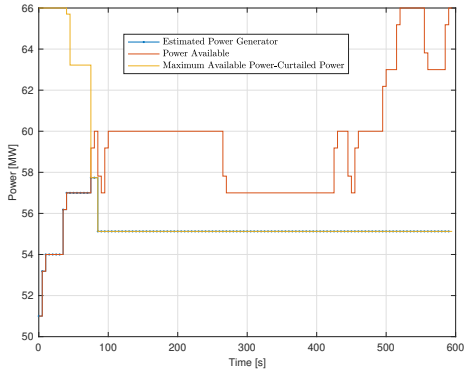

Fig. 4. The power variables in the power generator at node 2076 from the MPC result with prediction horizon N=10. The yellow one depicts $\overline{P}_n^G - P_n^C(k)$, the red line represents $P_n^A(k)$, and the dotted blue one is $P_n^G(k)$.

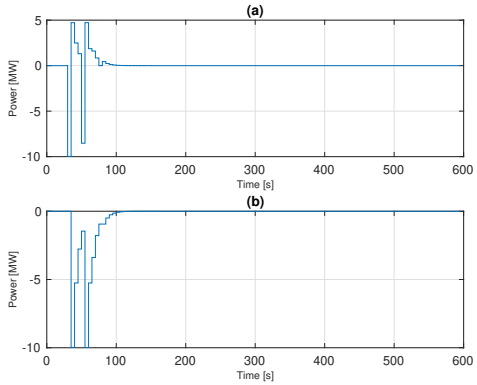

Fig. 5. (a): ΔP_n^B. (b): P_n^B. The prediction horizon is N=10.

as branches are equal to 0 as well:

$$\tilde{Q} = diag\{\mathbb{0}_{7\times7}\ 10^3{*}I_{4\times4}\ 10^{-3}{*}I_{1\times1}\ \mathbb{0}_{5\times5}\ 10^3{*}I_{28\times28}\ \mathbb{0}_{1\times1}\}. \tag{34}$$

Figure 4 depicts the power generated by the power plant in bus 2076 when the closed loop system with control inputs computed via MPC is considered, on the contrary to the open loop shown in Figure 2. The yellow line describes the maximum allowed power $\overline{P}_n^G - P_n^C(k)$, while the red one represents $P_n^A(k)$ and the dotted blue one is $P_n^G(k)$, with $n = 2076$. Between 0 and 90 s, the value of $P_n^G(k)$ is shown to track the value of $P_n^A(k)$, while after 90 s the condition in (3) forces $P_n^G(k)$ to track $\overline{P}_n^G - P_n^C(k)$.

The adopted control actions are depicted in Figures 5 and 6. Figure 5 describes the dynamical behaviour of the battery in node 10000, both in terms of power output variation and power output. Figure 6 describes the power curtailment variations. We remark that the figures show the sampling time the control inputs are calculated, and not the ones when they are applied.

From a comparison between the two control actions, we remark that the MPC privileges the use the battery before than curtailing, as desired. Moreover, the algorithm allows for a battery power charge reduction if possible, such to increase its capability to act on the system in the near future. While battery control action suffer of a delay of 1 sampling

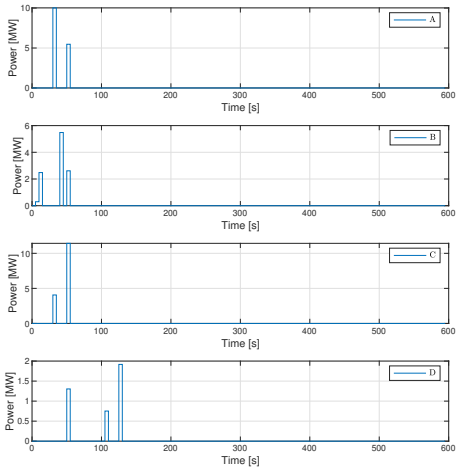

Fig. 6. ΔP_n^C at the generators. The prediction horizon is N=10. A) node 10000; B) node 2076; C) node 2745; D) node 4720.

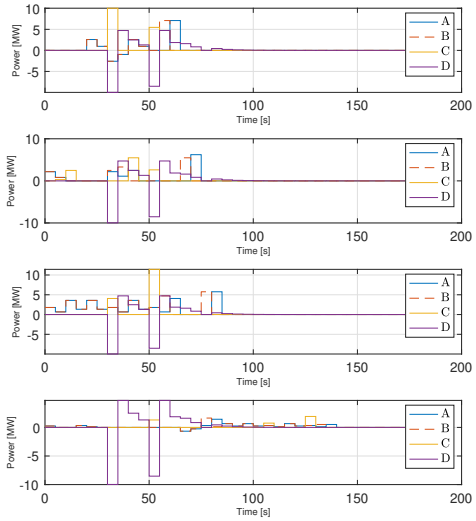

Fig. 7. ΔP_n^G at the generators 10000, 2076, 2745, and 4720. The prediction horizon is N=10. A) Real ΔP_n^G; B) Estimated ΔP_n^G; C) Curtailment action; D) Battery action.

time, the ones related to curtailment consider a time delay of 7 sampling times. However, it is possible to verify that some control actions take place quite early with respect to the constraints violations that are depicted in Figure 3. For example, the curtailment order in node 2076 acts very soon at $t = 5$ s, and at $t = 40$ s and $t = 50$ s. Motivations for this behavior can be found on the fact that the adopted prediction on ΔP_n^A is different from 0, and consequently the control algorithm adopts the needed countermeasures. With respect to this, Figure 7 describes the real values of the power generated variations ΔP_n^G with respect to the estimated ones.

According to the control actions depicted in the previous section, Figure 8 shows the effects of the closed loop system on the power flows on the same branches of Figure 3; as a

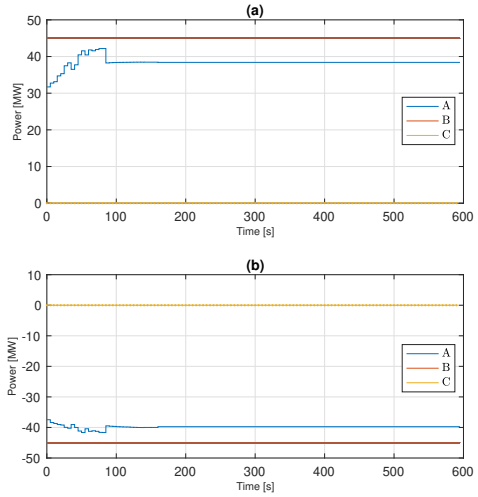

Fig. 8. The power flow on the branches in the closed-loop simulation: (a) between buses 2745 and 1445; (b) between buses 2135 and 2076. A) Power Flow in *runpf*. B) Limitation values for the branches. C) Epsilon values in soften constraints.

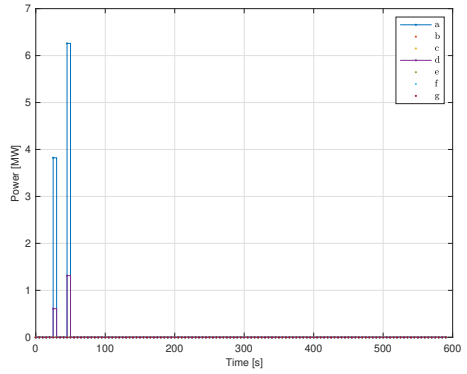

Fig. 9. Comparison of the values of slack variable ε for all branches in the sixth step of MPC prediction between: (a) buses 2745 and 1445; (b) buses 4720 and 1445; (c) buses 2745 and 1445; (d) buses 2135 and 2076; (e) buses 4720 and 2076; (f) buses 2745 and 10000; (g) buses 2076 and 10000.

result, they do not violate the constraints and are always inside the allowed power zone ranging from -45 MW to 45 MW. Figure 8 shows some differences with respect to Figure 3 already in the phase when only the battery lever is acting, i.e. between 0 s and 40 s. Then, when the power generated is saturated by the control action, the power flow is kept constant. We remind that the power flows are simulated by MATPOWER with respect to the power that is allowed to be generated by each power plant, according to the computed control inputs. A consequence of the uncertainty quantities in Figure 7 is the possible utilisation of the slack variables. Figure 9 depicts their values over the simulation time, and, since only 2 branches are shown to use slack variables to properly soften the constraints on the power flow, it motivates the choice to show only these branches in the previous figures.

V. Conclusions

In this paper, a receding horizon control approach is proposed based on an underactuated time-delay dynamical model of the power transmission network with the purpose to avoid power flow constraint violation. A sub-transmission power area is examined, and the possibilities to act on a storage device and partial curtailment of the renewable power are considered as control variables. A controllability analysis of the system is presented, and strategies to ensure problem feasibility and handle uncertainties are adopted. Simulations shows the effectiveness of the proposed control action.

References

[1] B. Meyer, J. Astic, P. Meyer, F. Sardou, C. Poumarede, N. Couturier, M. Fontaine, C. Lemaitre, J. Maeght, and C. Straub, "Power Transmission Technologies and Solutions: The Latest Advances at RTE, the French Transmission System Operator," *IEEE Power and Energy Magazine*, vol. 18, no. 2, pp. 43–52, 2020.

[2] A. Iovine, D.-T. Hoang, S. Olaru, J. Maeght, P. Panciatici, and M. Ruiz, "Modeling the partial renewable power curtailment for transmission network management," *2021 IEEE Madrid PowerTech*, pp. 1–6, 2021.

[3] A. J. Wood, B. F. Wollenberg, and G. B. Sheblé, *Power Generation, Operation, and Control, 3rd Edition*. Wiley, 2013.

[4] Xu Cheng and T. J. Overbye, "PTDF-based power system equivalents," *IEEE Transactions on Power Systems*, vol. 20, no. 4, pp. 1868–1876, 2005.

[5] C. Straub, S. Olaru, J. Maeght, and P. Panciatici, "Robust MPC for temperature management on electrical transmission lines," *IFAC-PapersOnLine*, vol. 51, no. 32, pp. 355 – 360, 2018, 17th IFAC Workshop on Control Applications of Optimization CAO 2018.

[6] ——, "Zonal congestion management mixing large battery storage systems and generation curtailment," *IEEE Conference on Control Technology and Applications (CCTA)*, pp. 988–995, 2018.

[7] D.-T. Hoang, S. Olaru, A. Iovine, J. Maeght, P. Panciatici, and M. Ruiz, "Predictive control for zonal congestion management of a transmission network," *2021 29th Mediterranean Conference on Control and Automation (MED)*, pp. 220–225, 2021.

[8] E. F. Camacho and C. Bordons, *Model predictive control*. Springer, 2007.

[9] M. V. Kothare, V. Balakrishnan, and M. Morari, "Robust constrained model predictive control using linear matrix inequalities," *Automatica*, vol. 32, no. 10, pp. 1361–1379, 1996.

[10] S. C. Jeong and P. Park, "Constrained MPC algorithm for uncertain time-varying systems with state-delay," *Transactions on Automatic Control*, vol. 50, no. 2, pp. 257–263, 2005.

[11] M.-T. Laraba, S. Olaru, and S.-I. Niculescu, "Linear model predictive control and time-delay implications," *IFAC-PapersOnLine*, vol. 50, no. 1, pp. 14 406–14 411, 2017.

[12] M. N. Zeilinger, M. Morari, and C. N. Jones, "Soft constrained model predictive control with robust stability guarantees," *IEEE Transactions on Automatic Control*, vol. 59, no. 5, pp. 1190–1202, 2014.

[13] R. D. Zimmerman, C. E. Murillo-Sánchez, and R. J. Thomas, "Matpower: Steady-state operations, planning, and analysis tools for power systems research and education," *IEEE Transactions on Power Systems*, vol. 26, no. 1, pp. 12–19, 2011.

[14] C. Josz, S. Fliscounakis, J. Maeght, and P. Panciatici, "AC Power Flow Data in MATPOWER and QCQP Format: iTesla, RTE Snapshots, and PEGASE," *arXiv, 1603.01533*, 2016.

[15] C. Straub, J. Maeght, C. Pache, P. Panciatici, and R. Rajagopal, "Congestion management within a multi-service scheduling coordination scheme for large battery storage systems," in *2019 IEEE Milan PowerTech*, 2019, pp. 1–6.

[16] J. Löfberg, "Yalmip : A toolbox for modeling and optimization in matlab," in *In Proceedings of the CACSD Conference*, Taipei, Taiwan, 2004.

[17] L. Gurobi Optimization, "Gurobi optimizer reference manual," 2021. [Online]. Available: http://www.gurobi.com